ELSEVIER

Journal of Structural Geology 29 (2007) 1148–1163

JOURNAL OF STRUCTURAL GEOLOGY

www.elsevier.com/locate/jsg

Development of crestal normal faults associated with deepwater fold growth

C.K. Morley*

172 Baan Yosawaadi, Pahonyohothin, Bangkok 10900, Thailand

Received 1 October 2006; received in revised form 28 March 2007; accepted 29 March 2007
Available online 14 April 2007

Abstract

Deepwater anticlines during their early stages of development (approximately between interlimb angles of 180° and 140°) grow and accumulate weak, fine grained and poorly lithified sediment on their crests. Growth of the anticlines induced gravitational instability within the syn-kinematic sediments and development of a range of shallow, gravity-driven failure mechanisms. In addition to shallow (tens of metres depth to detachment) rotational landslides, deeper seated normal fault swarms also affect the fold crests and upper fold limbs. These faults tend to penetrate to depths between 200 and 800 m, are 100s of metres to a few kilometres long, planar to weakly curved in cross-section and display throws in the order of tens of metres. The faults do not sole out into a detachment, but die out downwards. They can occur as single sets, or tiers of faults that have developed at different times. In map view the fault patterns range from straight to anastamosing to highly curved with complex cross-cutting relationships. The number and orientation of faults corresponds to the maximum slope dip and direction, and consequently the faults are inferred to be mainly the product of gravity induced deformation, although tangential stresses arising from outer arc bending of a fold or crestal collapse in response to a mobile sedimentary unit may contribute to some extent.

Keywords: Normal faults; Fold crest; Mass wasting; Syn-kinematic

1. Introduction

Fold development in deepwater (i.e. beyond the shelf-slope break, from about 200 m to 3+ km water depth) areas is characterised by syn-tectonic sediment deposition, and the impact of gravity-driven mass movement processes on growing anticlines. During the growth phase unlithified to poorly lithified, predominantly mud-prone sediments are deposited over the crests of growing anticlines. In the deepwater offshore area studied, crestal sediment accumulation occurs during the early stages of fold development, between fold interlimb angles of 180° and ~140°. During continued growth, as interlimb angles increase, these syn-kinematic sediments tend to be removed by slumping, erosion by currents and flows and affected by a range of gravity processes. Where these processes locally reduce the surface slope dip, deposition on top of the anticline crest can be renewed. These various processes have been discussed by Ingram et al. (2004), Nigro and Renda (2004) and Heinio and Davies (2006) and are described in detail by McGilvery and Cook (2003). One aspect of fold development seen in the deepwater 3D seismic data, are minor faults systems that run along the crests of anticlines. This paper describes the structural characteristics of these fault systems, that in places are spectacularly imaged by 3D seismic reflection data (Fig. 1).

Systems of small faults are commonly found affecting the crests of anticlines (Fig. 1), they are characterised by small vertical offsets ranging up to about 50 m, but more typically range between 10 m and 30 m. Many faults are at the limit of seismic resolution, however even where reflections are not offset, but just slightly kinked, the faults are commonly regions where the usual reflector amplitude is diminished, and on typical seismic displays the trace of the fault is marked by a narrow white, poorly reflective zone. Consequently the fault patterns can be imaged on amplitude maps, time slices and coherency cubes.

* Corresponding author. Tel.: +66 026131363.
E-mail address: chrissmorley@gmail.com

0191-8141/$ - see front matter © 2007 Elsevier Ltd. All rights reserved.
doi:10.1016/j.jsg.2007.03.016

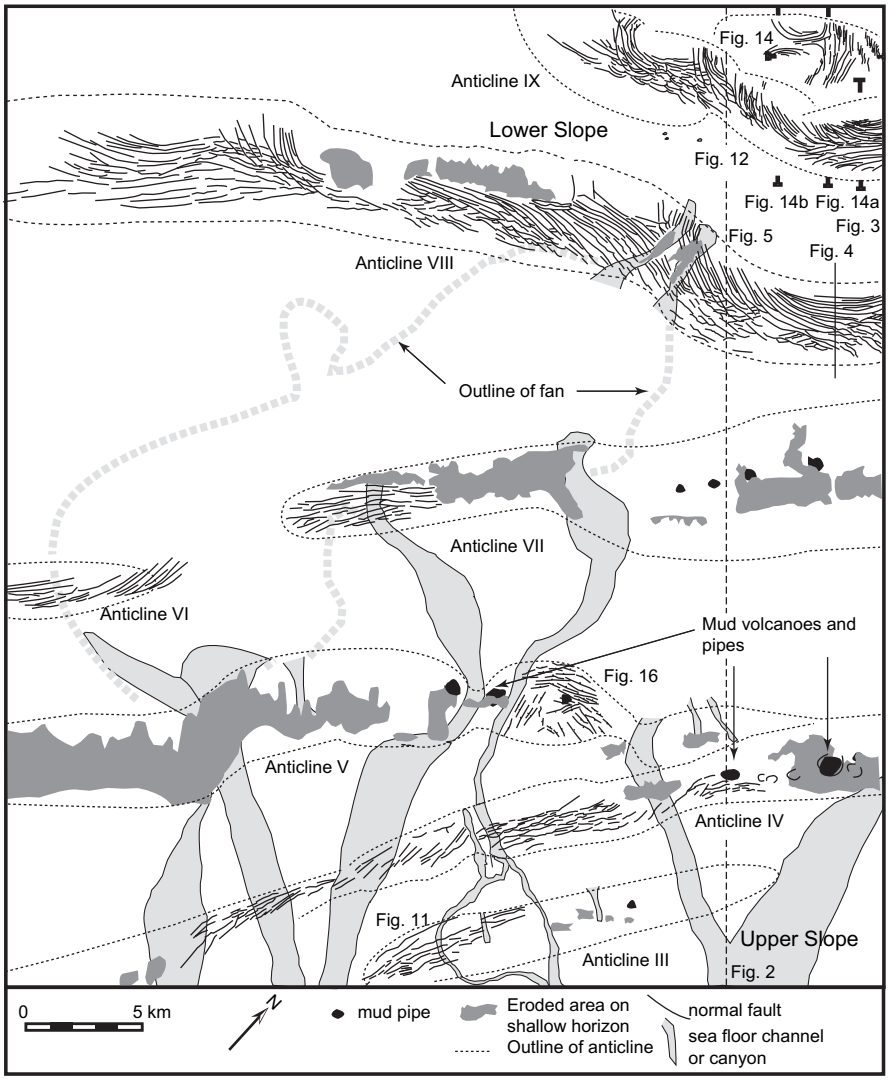

Fig. 1. Location map showing the main anticline trends in the study area and the normal fault patterns affecting their crests. The shallow normal fault patterns and regions of erosion affecting the shallow section are the result of gravity processes during fold growth. Patterns based on mapping of 3D seismic data. The outlines of the anticlines mark where the crests are uplifted above the general trend of the sea floor.

It is believed that this paper describes for the first time in detail the geometry and development of crestal normal faults associated with deepwater fold development.

2. Data

The seismic data is from a basin in SE Asia. The normal faults occur in the upper one second of data which would be approximately equivalent to 0.8–1 km depth of section, of predominantly poorly compacted Pliocene-Recent age. Generally around the anticline crest horizons were picked every 25 lines and traces using seismic interpretation (SeisWorks) software. However in some areas of high density faulting, lines and traces were picked every 2–10 lines. Line spacing is every 12.5 m, hence the spacing of the 25 × 25 grid is 312.5 m. The main mapped area is about 50 km in a strike direction (NE-SW) and up to 60 km in a dip direction (NW-SE). The final infill of the grid was conducted using an autopicker, to produce a continuous horizon. On vertical sections through the seismic data fault zones tend to show up as narrow zones of weak amplitudes. Hence the faults are associated with amplitude anomalies and show good definition on amplitude maps. To determine the sedimentation patterns and fault patterns in map view from amplitude anomalies, two methods were used: (1) the amplitude of the autopicked horizon, and (2) the root mean square (rms) of anomaly values for a 10 ms window of data sampled above or below an interpolated and smoothed version of the picked horizon using seismic amplitude mapping (StratAmp) software. Smoothing was used to obtain a good picture of the fault amplitude response by eliminating irregularities in the autopicked horizon in areas of intense faulting, where even with a close spacing of interpreted lines the autopicker encountered correlation problems. For further details of these methods see Brown (1996). Similar results were obtained using the different methods, but the clarity of fault definition varied.

2.1. Syn-kinematic sedimentation and fold growth

The crests of growing anticlines are generally uplifted above the regional height of the surface, unless the folds are in an environment where sedimentation rates are fast enough to cover the anticline as they grow. The way the growing folds interact with their environment occurs in different ways passing from continental to shallow marine to deep marine settings due to the variable nature of erosion and mass wasting processes, opportunity for burial, and lithology of rocks in the anticlines in these different environments. Continental settings (e.g. Zagros mountains; Colman-Saad, 1978; Burbank et al., 1999) display little deposition on the anticlines during growth, typically anticlinal crests are composed of well lithified rocks and uplift during folding subjects the crests to erosion and mass wasting. Any sedimentation that occurs in subaerially exposed anticlines onlaps the flanks and is deposited in the synclinal depocentres. An exception occurs when continental folds develop within a subsiding basin, usually a foredeep basin. In associated fill-to-the-top models (see review in Castelltort et al., 2004) sedimentation may keep up with fold growth and spare the crest from major erosional truncation (e.g. Apennines foredeep basin (Bally, 1989), modelling by Cooper et al., 2003). In a shallow marine environment the same gradation between the two cases discussed above occur. However in shallow marine conditions a greater opportunity exists for syn-kinematic sedimentation to occur than in the continental setting. The inner shelf fold crests that rise just a few tens of metres above the general depth of the sea floor, are liable to either wave, or sub-aerial erosion. Deepwater folds differ from the settings above for three main reasons: (1) folds are protected from sub-aerial and wave-related erosion, hence thicker, and more widely distributed syn-kinematic sedimentation can occur both across anticlines and within synclinal depocentres; (2) the syn-kinematic sediments deposited across anticlines are poorly lithified, predominantly fine-grained and weak, and hence deepwater anticlines are very sensitive to gravitational force during fold growth (e.g. Nigro and Renda, 2004; Heinio and Davies, 2006); and (3) the main erosional processes are a variety of mass movement phenomena, including rotational slides, fast and slow creep mass movement, debris flows, and turbidity flows, and currents (e.g. McGilvery and Cook, 2003; Ferguson et al., 2004; Heinio and Davies, 2006).

Typically in deepwater fold belts the upper continental slope folds are covered by post-kinematic sediments, whilst at the foot of the slope the seafloor is buckled and uplifted by growing anticlines (e.g. James, 1984; Hinz and Schluter, 1985; Hinz et al., 1989; Sandal, 1996; Demyttenacre et al., 2000; McGilvery and Cook, 2003; Ping and Liu, 2004; Ingram et al., 2004; Ferguson et al., 2004). Isopach patterns of different syn-kinematic units of the studied fold belt shows an overall pattern of younging offshore of a broad belt of folds (typically about five major folds wide, i.e. ~40–50 km width) that is or was active at any one time. Anticline-related sea floor ridges show an increase in the effects and variety of mass movement and gravity processes landwards (Demyttenacre et al., 2000; McGilvery and Cook, 2003). The youngest, most external folds (lower slope) show an almost pristine fold shape, with a convex upwards seafloor profile. The upper slope folds either have no associated sea floor topography due to sediment infilling of topography, or form sea floor ridges that are highly modified from the original fold shape by mass wasting processes (Fig. 2). Eroded ridges are affected by mass movement processes, including focussing of turbidites into channels, which dissect the once long, linear ridges into short segments (Fig. 1). In places the channels disappear, and are replaced by fans in synclinal basins. However upon exiting the synclines flow can become locally focussed again, for example in the structural low (saddle) between the two segments of anticline VIII two channels are present cross-cutting the anticline (Fig. 1).

2.2. Cross-section geometries

The deepwater folds typically verge downslope, back-limb and forelimb are defined with respect to the general vergence. In cross-sections the normal faults located towards the fold axis generally have upper and lower fault tips that lie at deeper levels with respect to faults located towards the forelimb (Figs. 3 and 4). When conjugate fault sets occur they are commonly transitional between back-limb dipping and forelimb dipping sets of synthetic faults. Particularly with the conjugate fault sets it is possible to see vertical tiers of fault sets, where

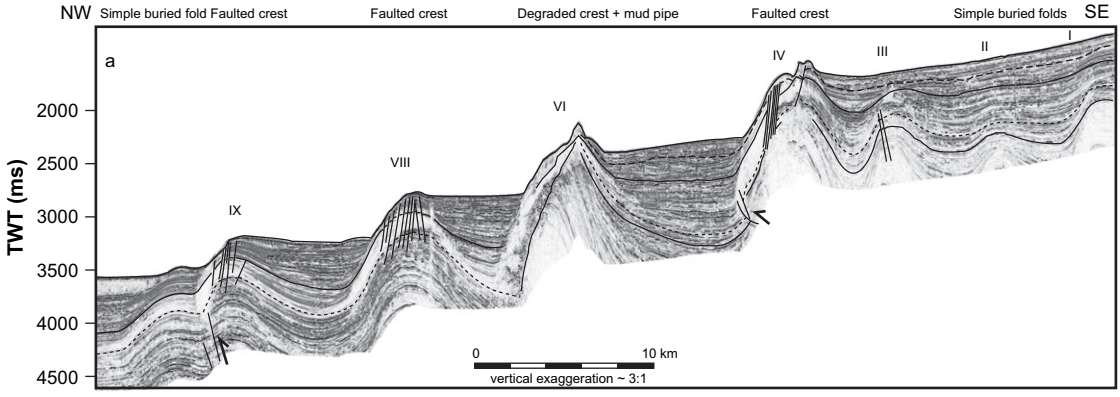

Fig. 2. Regional seismic line (clipped at 1 s below the sea floor) showing the varying styles of fold geometry across the area. Faulted crest anticlines, are affected by the normal faults discussed in this paper. See Fig. 1 for location.

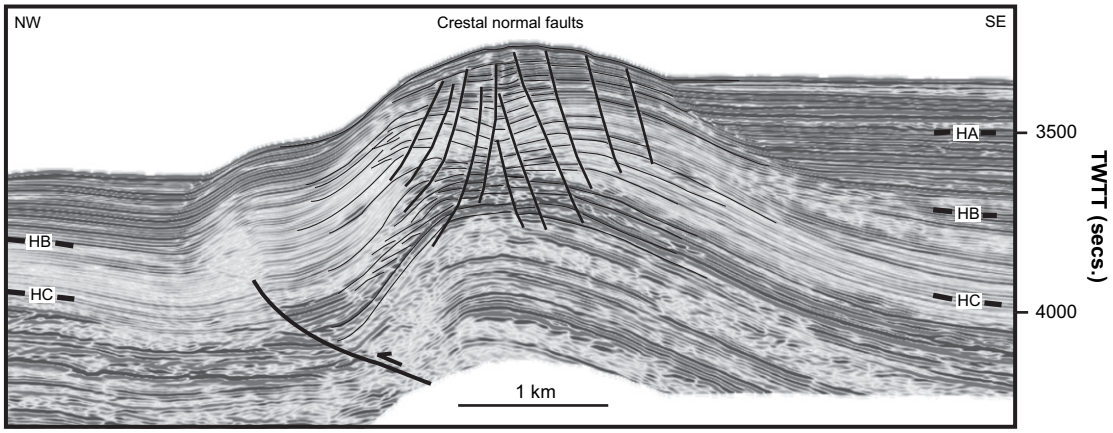

Fig. 3. Seismic line across the most external anticline (IX), showing that the seafloor is folded quasi-conformably with more internal reflections. See Fig. 1 for location.

two to four different fault sets are stacked on top of each other (Fig. 5). Some of the biggest faults traverse all the tiers, probably as a result of vertical linkage of earlier faults with later faults.

In cross-section faults display throws up to 50 m, and die out downwards and upwards or reach the sea floor. They are planar to slightly curved, and dip between about 60° and 40°. Synthetic groups of faults cause rotation of beds in a modified domino fault style but do not sole out into a master detachment, instead the faults die out downwards. The rotation is achieved by higher displacements towards the middle of the fault (e.g., Fig. 2). Rarely the faults are more strongly rotational and sole out into a detachment. However, the detachment does not pass down-dip into any detectable debris flow, or toe thrusts.

The faults range in vertical height from about 200 m to 800 m. Backlimb-dipping faults occur less frequently than forelimb-dipping faults. Fault sets can be entirely composed of forelimb-dipping faults, but rarely entirely of backlimb-dipping ones. Where backlimb-dipping faults are present the cross-section pattern is one of conjugate fault sets (Figs. 5 and 6) or separate divergent fault sets (Fig. 3).

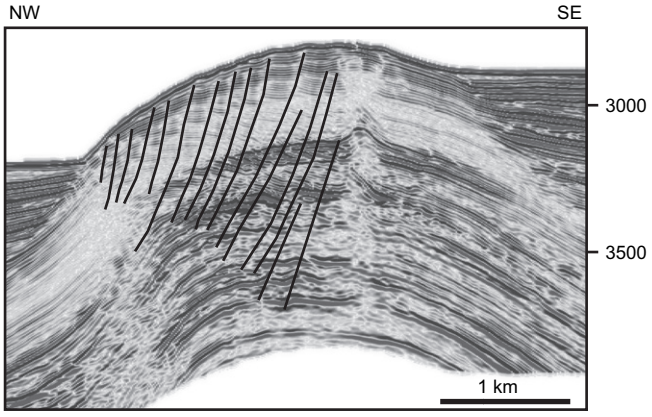

Fig. 4. Example of forelimb-dipping normal faults, anticline XIII. The faults young to the NW, and systematically terminate at shallower depths in the same direction. Note small gas pipe at fold crest.

Forelimb-dipping fault arrays can contain up to 30 faults that are visible on seismic data. Typically the faults towards the crest are the deepest (penetrating down to about 800 m), whilst the sets furthest towards the forelimb are the shortest and shallowest (penetrating down to 200 m; Figs. 3, 4 and 7). The location of upper and lower fault tips progressively higher in the section passing towards the forelimb indicates the faults tend to young towards the forelimb.

Probably some vertically stacked faults developed simultaneously, perhaps due to variations in mechanical stratigraphy. However the poorly lithified and mud-prone nature of the shallow stratigraphy suggests mechanical contrasts are unlikely to be great. More common is evidence for faults sets of different age developed during different phases of folding, hence deeper, older faults, and younger higher faults can be stacked vertically. Fig. 5 illustrates such a vertical stacking pattern where early conjugate fault sets were developed below the dashed horizon, a subsequent phase of folding then generated the second set of higher faults. During the second phase some of the older faults were reactivated, or became vertically linked with younger faults. Dip displacement patterns on some faults show either multiple displacement peaks, or broad zones of similar displacement values (Fig. 8, Trace 9397) which support the vertical linkage patterns observed in Fig. 5. Their displacement patterns are distinct from the majority of faults which show a single displacement maxima, with an asymmetric displacement profile (Fig. 8).

As fold growth continued the tighter anticlines became more prone to deep erosion, consequently much of the section containing early-formed normal faults has been eroded off. When sediment was deposited above the angular unconformity new normal faults formed, or the remaining segments of older faults were reactivated. In the comparatively mature regions of folds multiple angular unconformities are present (Fig. 7b,c). A typical range of fault geometries is illustrated in Fig. 9.

The crests of anticlines, particularly the more mature ones are the sites of considerable fluid activity (Fig. 9d). This is seen by the presence of several features on seismic data: (1) bottom simulating multiples indicative of gas hydrates, (2) vertically stacked high amplitudes on one side of a normal

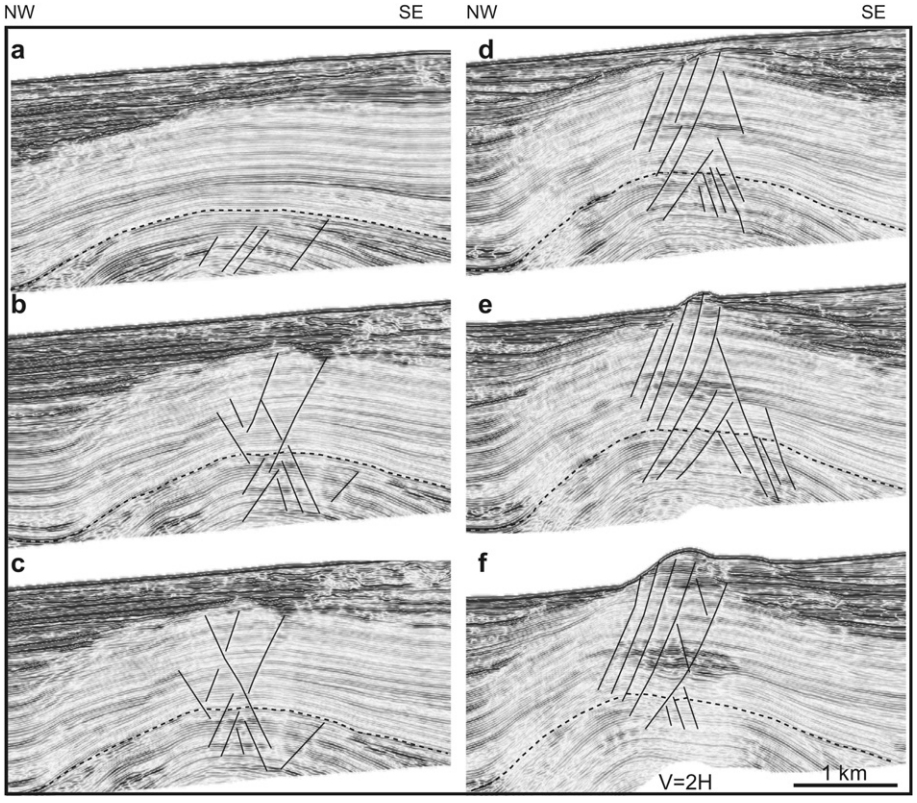

Fig. 5. Series of dip sections along anticline III showing conjugate fault sets developing in tiers, and the progressive increase in complexity of fault patterns passing towards the anticline crest. See Fig. 11 for location. Dashed line follows a marker horizon that approximately separates the oldest set of faults from the younger one.

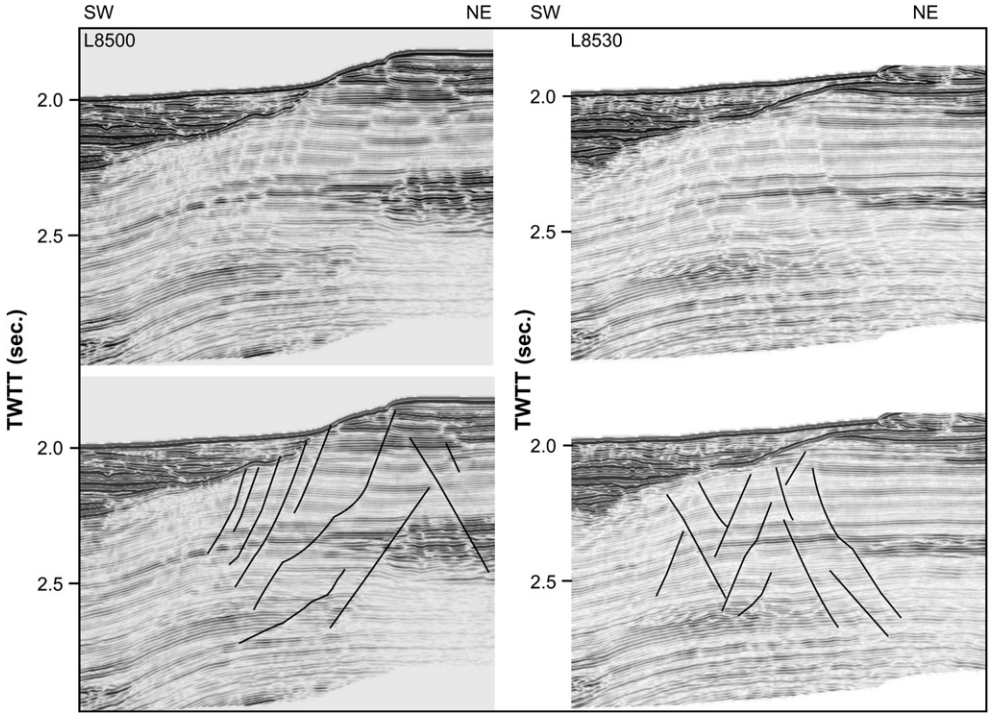

Fig. 6. Two strike-lines along anticline III illustrating normal fault patterns. See Fig. 1 for location.

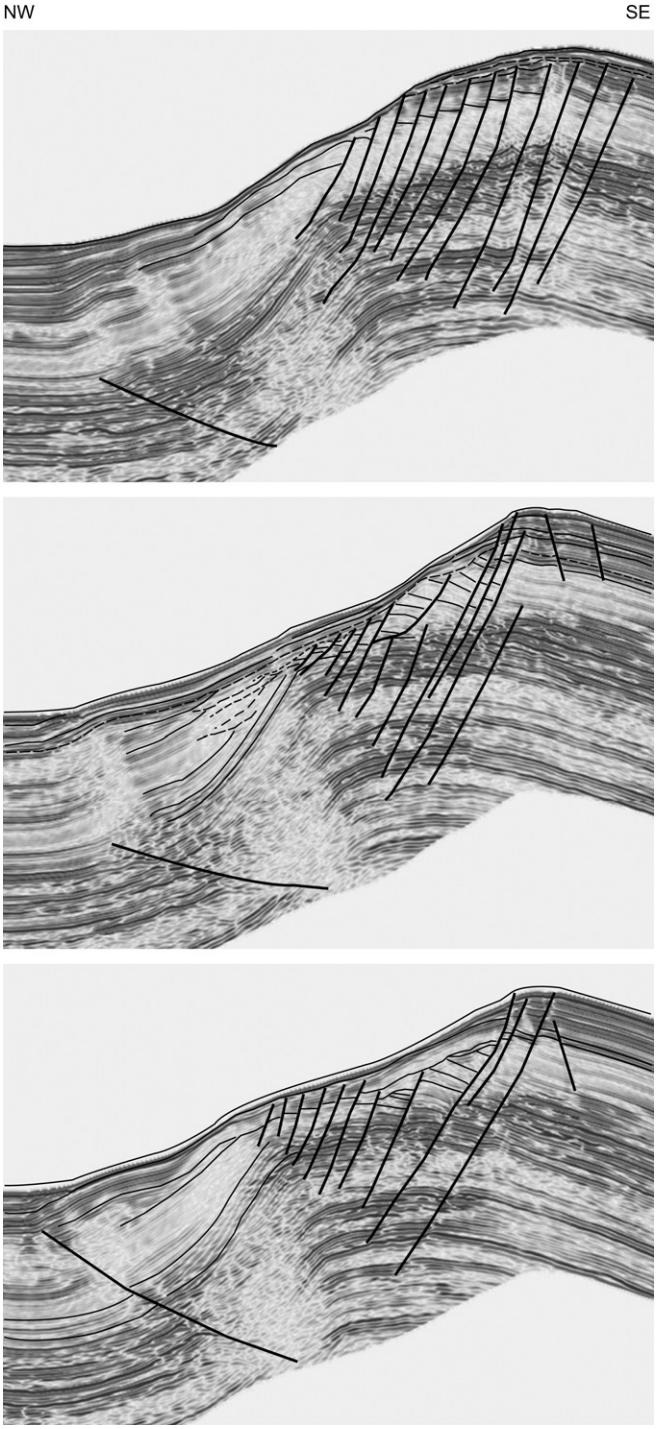

Fig. 7. Seismic lines across anticline VIII showing rotational slide affecting forelimb of anticline, also affected by deeper-penetrating and more planar normal faults. See Fig. 1 for location.

fault (possible gas-charged units), (3) narrow pipe like features associated with velocity pull-ups (inferred gas chimney), (4) larger pipe like features up to 1 km across (inferred mud pipes), (5) narrow pipe like features with collapse geometries (inferred fluid-escape pipe). It is difficult to map normal fault geometries in these regions, hence the illustrations provided here are from the simpler regions of folds.

2.3. Map view patterns

Where the normal faults affecting the anticlines are widely spaced they die out upwards, downwards and laterally with a classic isolated fault geometry (e.g. Walsh and Watterson, 1988; Cowie and Scholz, 1992; Nicol et al., 1996). Towards fault tips, one or several synthetic fault segments tend to develop and displacement is transferred between them in either hard-linked or soft linked geometries. Fault length for widely spaced 30 m displacement faults is typically a maximum of 1–2 km, (particularly for backlimb-dipping faults). The largest isolated faults in areas of more closely spaced faulting display maximum dimensions of 30–50 m displacement, strike lengths between 3 and 5 km (Figs. 10, 11), and fault dip-lengths between 600 and 800 m. This length–displacement ratio is 100:1 or greater, much larger than the more typical ratio of 10:1 to 20:1 for average fault populations (e.g. Walsh and Watterson, 1988; Nicol et al., 1996; Fig. 10). The exceptionally long faults such as those in Fig. 11 arise from lateral linkage of relatively large faults. Linkage geometries are identified where faults with arcuate segments in map view meet and are very apparent from amplitude maps of the faults (Figs. 12b, 13). Linkage is common due to the closely spaced nature of the fault swarms which enhances the likelihood of faults joining along-strike. There does not appear to be any vertical restriction to fault growth, as the faults tend to die out at different depths, not at a consistent horizon, depth, or detachment.

Commonly fault patterns involve sub-parallel to anastamosing sets of faults developed around the crestal areas of folds, that lie sub-parallel to the fold axis (Fig. 1). Approaching the plunging noses of folds, interlimb angle decreases and the folds become broader. Consequently faults are fewer and tend to form divergent splays in map view where forelimb- and backlimb-dipping faults are present, and a gently curved fault pattern where just the forelimb-dipping faults are present (anticline VIIIb, Fig. 13). En-echelon fault patterns are also present in some areas (Fig. 1). There is considerable variety to the fault patterns, with a number factors affecting fault geometry.

The most external anticline (IX; Fig. 13) is affected by comparatively normal few faults, and has a large interlimb angle, (180–160°) yet still shows a range of normal fault geometries. The northeastern part of the fold is affected by faults sub-perpendicular to the strike of the fold; this is because the dip of the fold limbs is very small (Fig. 13), but the plunge of the fold to the NE is more pronounced (Fig. 14). This example clearly shows that the fault orientations respond to dip of the layers. A more complex example is shown in Fig. 15 where three main orientations of faults are present, a NE-SW trend that is parallel to the fold forelimb, an E-W trend that lies parallel to the plunging nose of the anticline to the NE, and a N-S trend. The N-S trend occurs locally parallel to a canyon cutting across the crest of the anticline where it was weakened by intrusion of a mud pipe. This indicates the fault orientation was responding to the N-S trending (west-dipping) slope cut by the canyon.

Another aspect of fault modification are shallow rotational slides, in addition to the steep normal faults fold forelimbs are

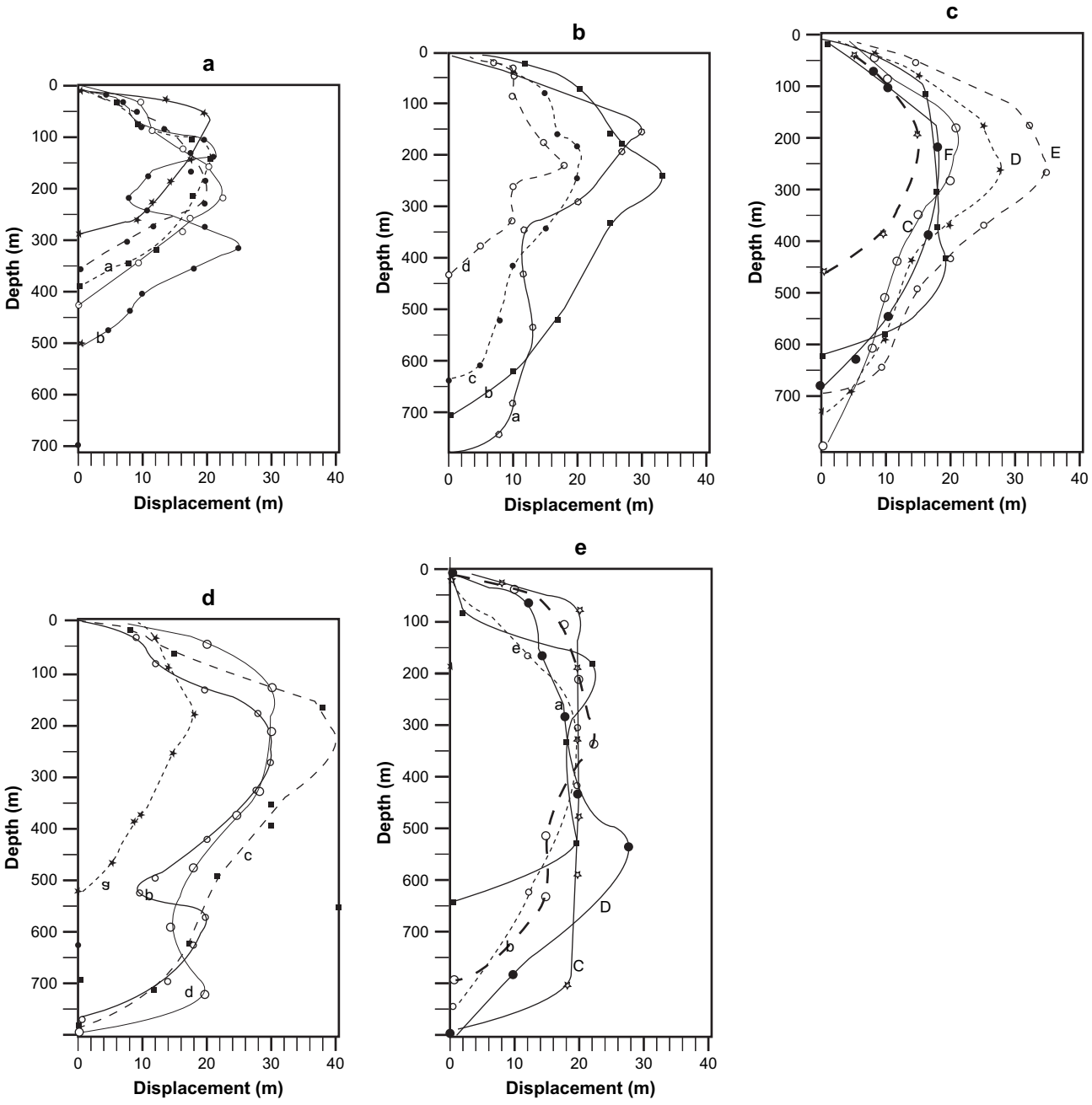

Fig. 8. Displacement profiles in dip-sections of normal faults. The profiles come from dip-section seismic lines, where the following criteria were met: (1) reflection characteristics could be readily correlated across faults, (2) some of the fault geometry was not obscured by the effects of gas and gas hydrates, and (3) the tops of faults were not eroded. These criteria limited the number of faults that could be used significantly.

commonly affected by rotational slides, that tend to detach parallel to the steep forelimb slope at depths of about 100 m or less (Fig. 7). These slides are linked with extensional faults up dip, and folds and thrusts at the down dip termination of the slide. Fig. 12a shows an edge map of the seafloor where slump scars are breaking up a forelimb also affected by the non-detachment normal faults. An amplitude map of horizon B (Fig. 12b) shows the deeper fault pattern within the anticlines. The result of the interaction between slumps and normal faults produces an angular discordance between the seafloor reflection and the internal reflections of the fold (Figs. 8, 9 and 17). There can be multiple unconformity surfaces within the normally faulted sequence, indicating repetition of the faulting and slumping process during fold growth (Fig. 17). Landslides produce depressions, benches and bulges in the slope that modify the overall convex-up geometry (Fig. 12a, locations a and c). The strongly curved map-view fault patterns in Fig. 12 occur at the edge of the rotation slide area, indicating that the shallow stresses associated with slump-induced topography caused the change in fault strike, to produce the arcuate fault pattern.

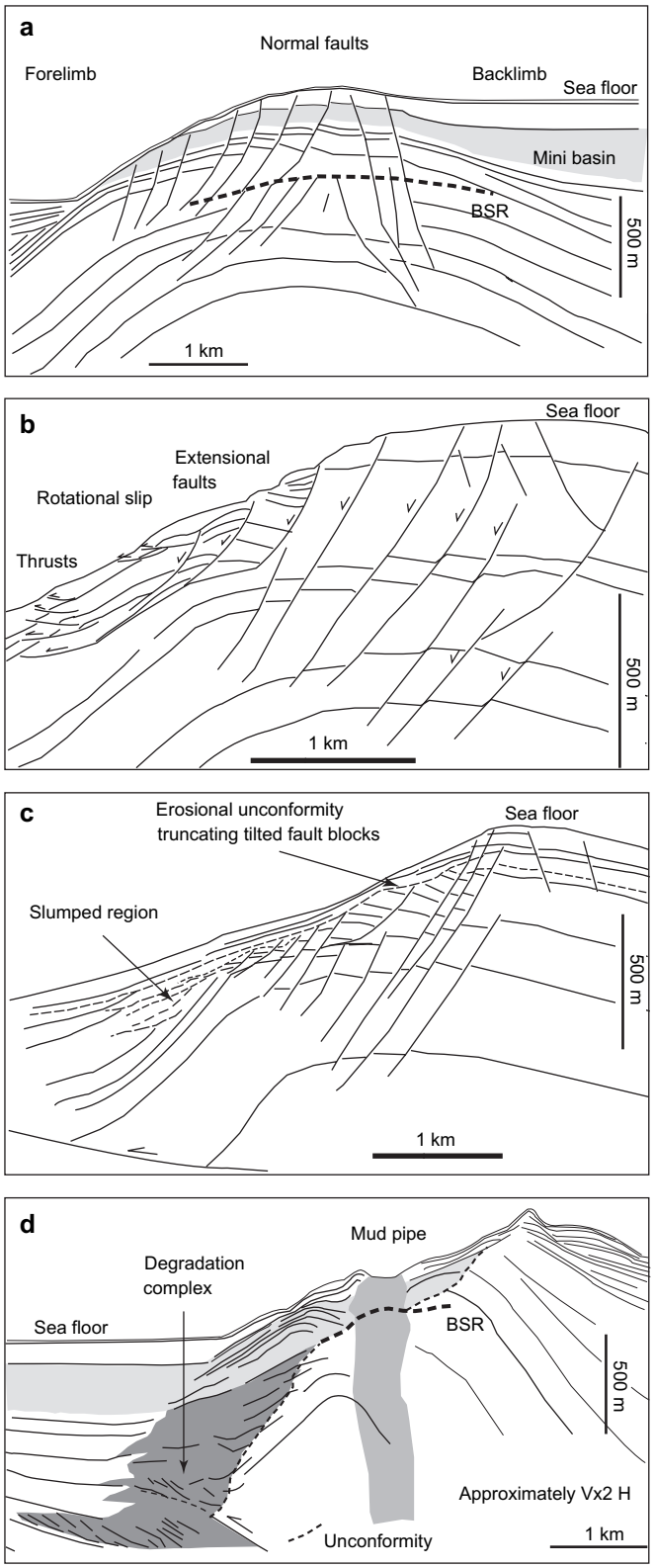

Fig. 9. Sketches (based on geometries observed on 3D seismic data) of the range of fold styles developed during anticline growth and decrease of interlimb angle from 180° to 140°: (a) fold with normal faults; (b) fold with normal faults and rotational slide; (c) fold with normal faults and multiple rotational slides leading to shallow angular unconformities; (d) fold with degradation complexes and mud pipe.

2.4. Fault interference patterns

Cross-cutting fault relationships are apparent in a number of places along folds (Figs. 1, 12, 13) and generally tend to follow the pattern of older fold axis sub-parallel faults being cut by faults that have a strongly oblique strike to the fold axis. These relationships appear most to occur under two conditions (Fig. 18): during fold amplification where the interlimb angle decreases (Fig. 18c), and during lateral fold propagation and linkage of en-echelon anticlines (Fig. 18d). As discussed above the increase in fold amplitude is accompanied by an increase in mass wasting, surrounding these areas can be a strongly arcuate fault pattern, which is significantly different in orientation from, and cross-cuts the earlier fold axis sub-parallel pattern (Fig. 12, with details of cross-cutting relationships in insets c and d). The fault pattern is reminiscent of the arcuate geometry of rotational slides.

Two variations on the propagating fold theme are seen in the study area: one is where normal faults lie sub-parallel to the local fold axis orientation, the other is where normal faults strike in sub-perpendicular orientations to the plunge direction of the fold axis. Where en-echelon anticlines are present the fold axes at the tips of the folds deviate into a trend oblique to the overall fold trend, normal faults also change orientation

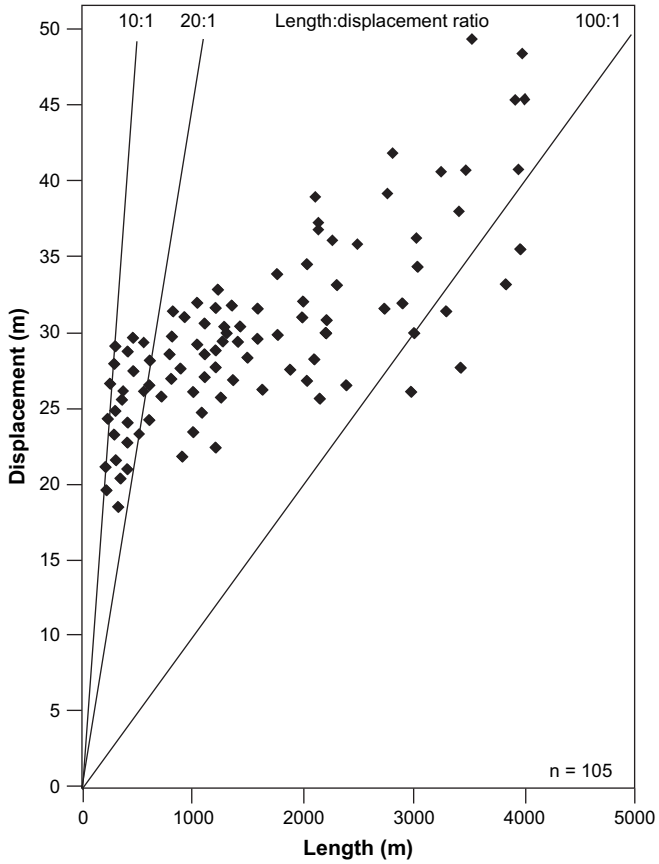

Fig. 10. Plots of normal fault length vs displacement for faults from anticline IX, illustrating the large range of fault length for a small variation in fault displacement. The broad scatter of data indicates numerous small faults linked during lateral fault propagation.

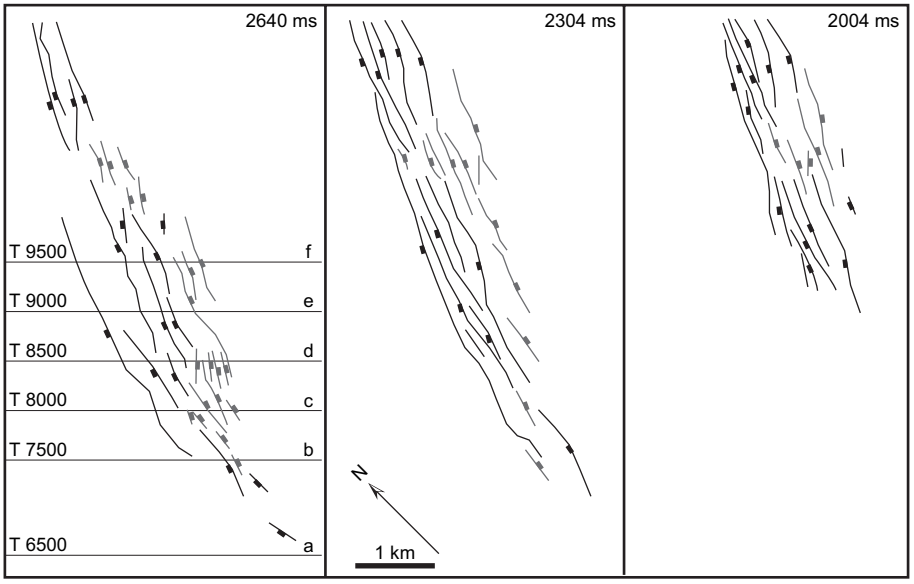

Fig. 11. Normal fault patterns from time slices through anticline III. The time slices illustrate lateral and vertical changes in normal fault geometry. The older faults occur more extensively along the anticline, younger faults are more confined to the crestal areas. See Fig. 1 for location.

and may lie sub-parallel to the oblique fold axis (Fig. 18d), or lie perpendicular (Fig. 18e) to the main fold axis. These later normal faults which tend to follow the oblique trend may cross-cut earlier less oblique normal faults (Figs. 12b,c, 18d).

Faults sub-perpendicular or highly oblique to the fold plunge direction are seen in three localities along the external anticline (IX) (Figs. 12, 13 and 19). Each one corresponds with an oblique ramp in the bounding thrust, the largest of which occurs at location a (Fig. 13). The cross-cutting relationships give some indication as to how fold propagation developed in the structure (Fig. 19).

2.5. Transfer of fault displacement to the surrounding rock volume

The normal faults die out both downwards and upwards in the section without passing into a deeper detachment. Most examples of fault displacement measured from seismic reflection data show a distinct asymmetry to the displacement pattern, with faults dying out upwards across a shorter distance from the displacement maxima than downwards. One exception are the examples of Fig. 8e which show unusual displacement patterns compared with Fig. 8a–d, and the upper fault segments have been eroded, hence this example is discounted for the moment. The other examples show a displacement peak between 150 and 250 m (Fig. 8a–d). Displacement gradients for the upper tip range between 0.8 and 2, clustering between 0.5 and 1. For the lower tip they range between 0.44 and 1.4, clustering around 0.44 to 1.2 (Fig. 20). A variety of factors may contribute to the displacement pattern including transfer between faults, minor growth of sedimentary section and compaction.

Deepwater sediments undergo greatest compaction from the surface down to about 200 m, followed by more gradual and uniform porosity loss with increasing depth (Cavin et al., 2000). Hence one explanation for the vertical displacement asymmetry is that loss of fault displacement by strain accommodation in the country rock is easiest in the upper 200 m, where porosity can be very high (60–70%) and faulting may cause bulk strain of the surrounding rock by dewatering and compaction. Thus fault tip gradients are higher for the upper segments of faults than the lower segments. Probably this displacement loss by bulk compaction of the adjacent sediment volume is achieved both by distributed deformation, particularly in finer-grained units and by formation of deformation bands in coarser-grained units. Such shallow level deformation bands in sand-prone units have been described from outcrops by Burhannudinnur and Morley (1997) and Cashman and Cashman (2000).

2.6. Origin of the faults

Normal faults are generated by anticline growth in a number of ways including: (1) extension in the outer arc of a fold due to bending stresses (e.g. Ramsay, 1967; Strayer et al., 2004); (2) collapse features due to withdrawal of a mobile unit or intrusions such as salt or overpressured clays; (3) a component of strike-slip or oblique slip motion acting along the anticline; or (4) as gravity slides associated with the topography and limb dips of growing, uplifting folds at the Earth's surface (e.g., Colman-Saad, 1978). The problems with interpreting the faults described here as being associated with outer arc extension include: (1) faulting is often as intense in the younger, less folded syn-kinematic strata than in the older, more strongly folded syn-kinematic strata; (2) fault strike appear to be related more to the maximum dip direction of near surface strata, than to deeper-seated fold geometry; (3) the dominance of faults that dip from the crest towards the forelimb does not fit crestal collapse models or outer arc extension, both of which would tend to display more convergent conjugate fault patterns (as illustrated by Strayer et al., 2004; Fig. 18f1); and (4) buried anticlines with strong curvature would be expected to show extensional faults

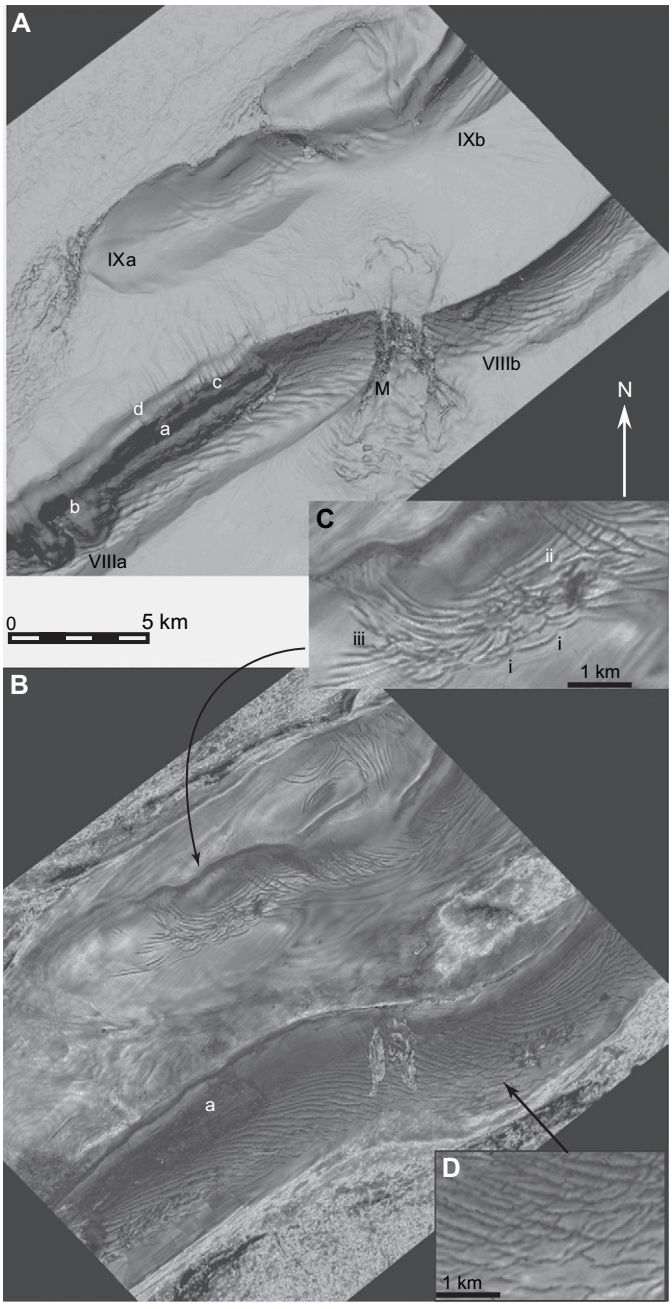

Fig. 12. (A) Edge map of the seafloor reflection showing normal faults (numerous dark lines) and slumped area associated with the external anticlines (IX and VIII), (see Fig. 1 for location): a, upper ridge associated with extensional rotation in the upper part of a major rotational slide; b, most intense region of mass movement cutting back high into the fold crest at the apex of the fold; c, ridge associated with toe thrust and fold region of slide; d, anticlinal ridge at tip of imbricate thrust fault (deep penetrating); M, region where canyons cut across fold saddle area. (B) RMS amplitude map of horizon B. The rotational slide region of area a disturbs the regular pattern of deep-penetrating normal faults seen beyond area a. Note the curvature of faults into the saddle region where two initially en-echelon anticlines (VIIIa and VIIIb) have propagated together and linked. (C) Detail of anticline IXa showing: (i) incipient linkage of small fault segments with curved tips, (ii) cross-cutting of fold axis sub-parallel fault set by later oblique fault, related to strongly NE plunging fault nose, and (iii) strongly listric faults cross-cutting earlier fold axis parallel faults inferred to be due to growth of the fold crest (Fig. 18c). (D) Detail of anticline VIII showing cross-cutting relationship between later NW-SE striking faults and earlier NE-SW striking faults. In places the NW-SE faults curve into and reactivate the NE-SW faults. Zoom into pdf figure to see details of fault pattern.

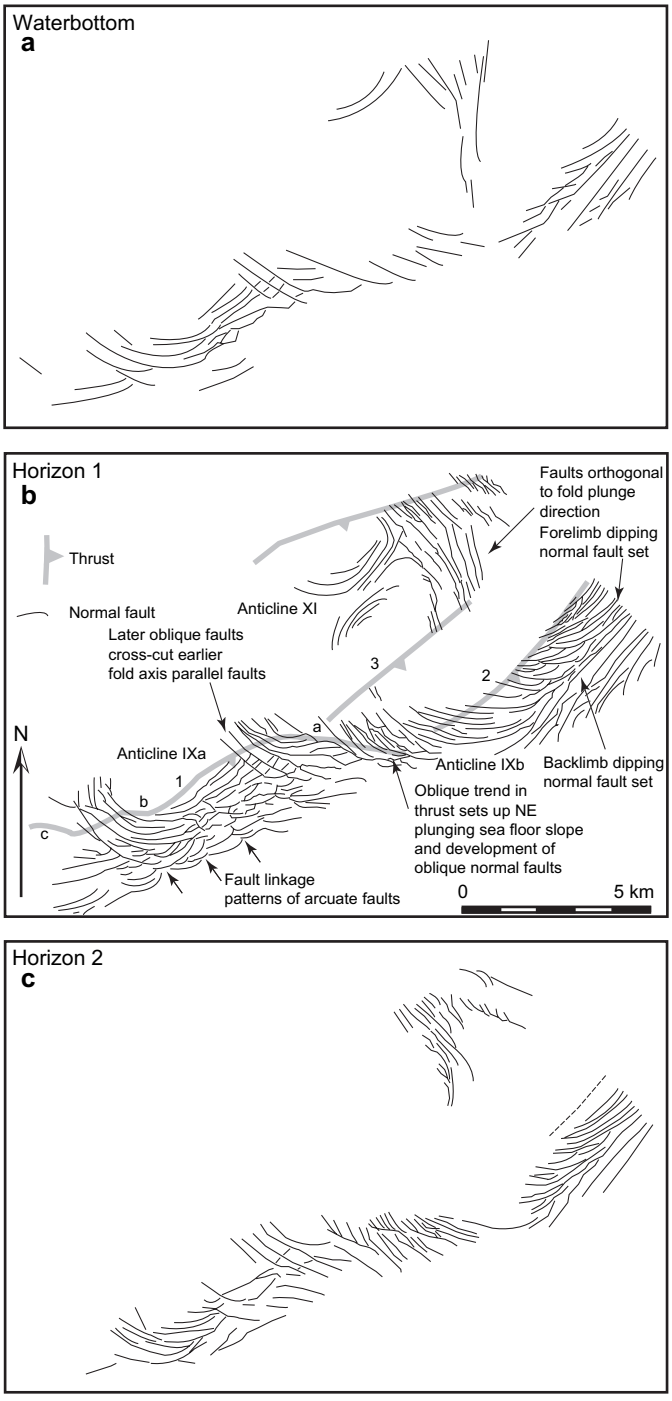

Fig. 13. Normal fault patterns based on amplitude maps associated with the most external anticline (Fig. 12). The numbers of faults decrease both upward and downwards from horizon 1. Horizon 2 is the deepest horizon thrust and fold geometry affect the strike direction of the normal faults. See Fig. 1 for location.

if bending stresses were the primary driving mechanism for faulting. However as shown in Fig. 2 there are buried anticlines with no faulting suggesting it is their lack of elevation above the regional sea floor trend that is significant, not their curvature.

Crestal faults associated with a component of strike-slip motion being present during fold development are not well documented in the literature, but some examples of folds

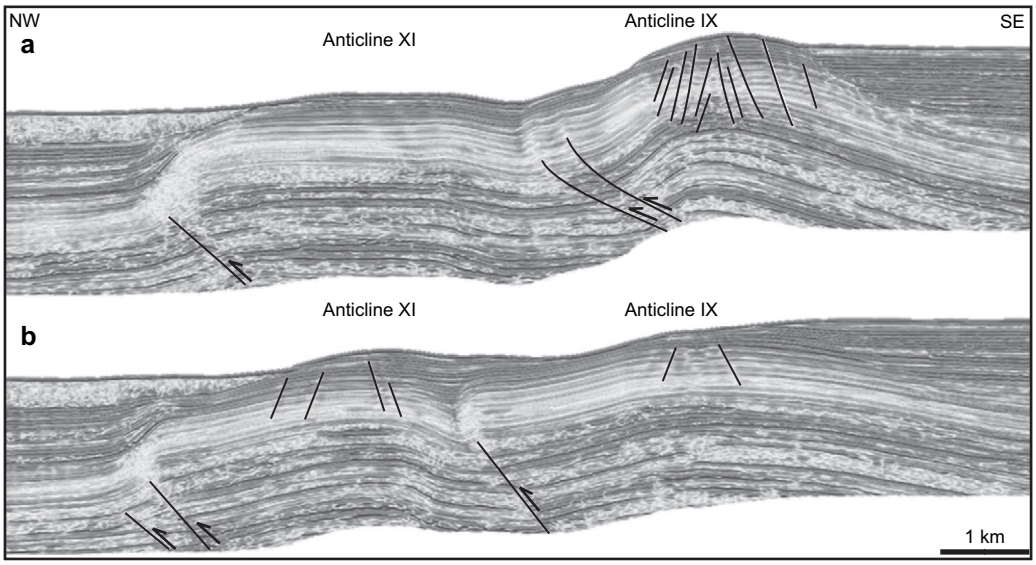

Fig. 14. Dip sections along anticlines IX and XI illustrating the fold geometry, which can be related to changes in normal fault geometry. See Fig. 1 for location.

associated with inversion along oblique structural trends around Brunei are presented in Sandal (1996). Within unpublished industry data the author is aware of examples of anticline crests affected by minor faults sets with a tendency to conjugate convergent geometries, that lie in trends parallel and oblique to the trend of the fold axis (illustrated schematically in Fig. 18f). Such fault geometries suggest that the combination of fold-related (local) bending stresses and regional maximum horizontal stress oblique to the trend of the fold axis have interacted to produce the oblique fault trends. In the examples of normal fault trends oblique to the trend of the anticlines in Fig. 1 there is no systematic oblique orientation displayed. In anticline VIII for example the oblique trends occur where there is an oblique orientation to the fold trend, in a saddle area where two propagating anticlines have met. In other examples such as anticline 1X(a,b), (Fig. 10b), the oblique trends show: (1) divergent orientations between the forelimb and backlimb areas; (2) an arcuate geometry similar to rotational slides; or (3) lie oblique or perpendicular to plunging fold terminations.

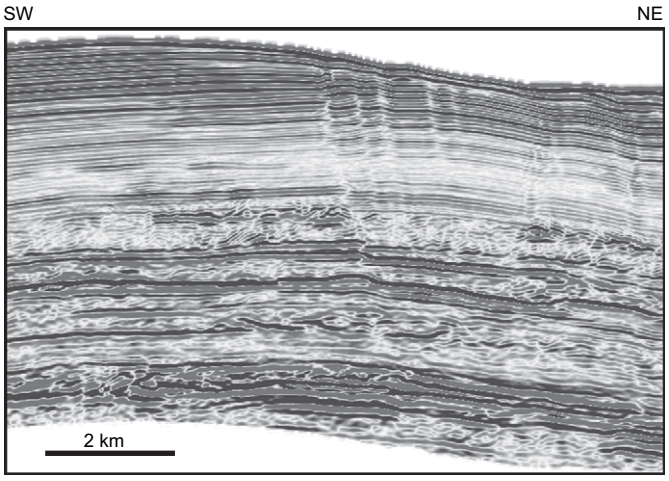

Fig. 15. Strike section along anticline XI where normal faults trend perpendicular to the fold axis. Comparing the section with Fig. 14, the surface downplunge dip seen on the strike section is greater than the dip in the dip direction (Fig. 14a). This demonstrates the control of surface slope on normal fault orientation.

Generally collapse features occur around circular or oval vents and diapirs, and can be characterised by both radial and concentric fault patterns (see Stewart and Davies (2006) for a recent review). Faults dips tend to converge with depth into the source of the volume collapse. These patterns are different from the long, linear fault patterns seen, for example in anticline VIII, which predominantly has faults that dip seawards, in the same direction as the forelimb.

Deep seated gravity sliding or shallow landslide mechanisms do not seem appropriate because the faults associated with these processes sole out into a detachment zone, and typically pass into toe folds or debris flows. Instead most of the faults observed around the anticlines are either planar and die out downwards at different depths and horizons, or more rarely they are listric, but do not pass into an extensive detachment. Passing along individual folds the number of faults increases as fold amplitude increases (Figs. 1 and 5). Whilst conjugate fault sets do exist, most faults dip in the direction of the more steeply dipping forelimb. These patterns, and the response of fault strike to slope steepening by mass movement and mass wasting suggests that gravity is the primary driving mechanism and that bending stresses only play a secondary role. The normal faults can be regarded as a deep seated, non-basal slide, mass movement phenomena. The faults occur within a range of gravity-induced phenomena that affect folds as they progressively tighten and increase in amplitude. The geometries range from simple faults at the highest interlimb angles, through normal fault-affected fold crests, fold crests affected by extensive landslides and normal faults, to at the smallest interlimb angles fold crests affected by degradation complexes, and multiple angular unconformities (Figs. 7 and 9). The context of fold–thrust–mass

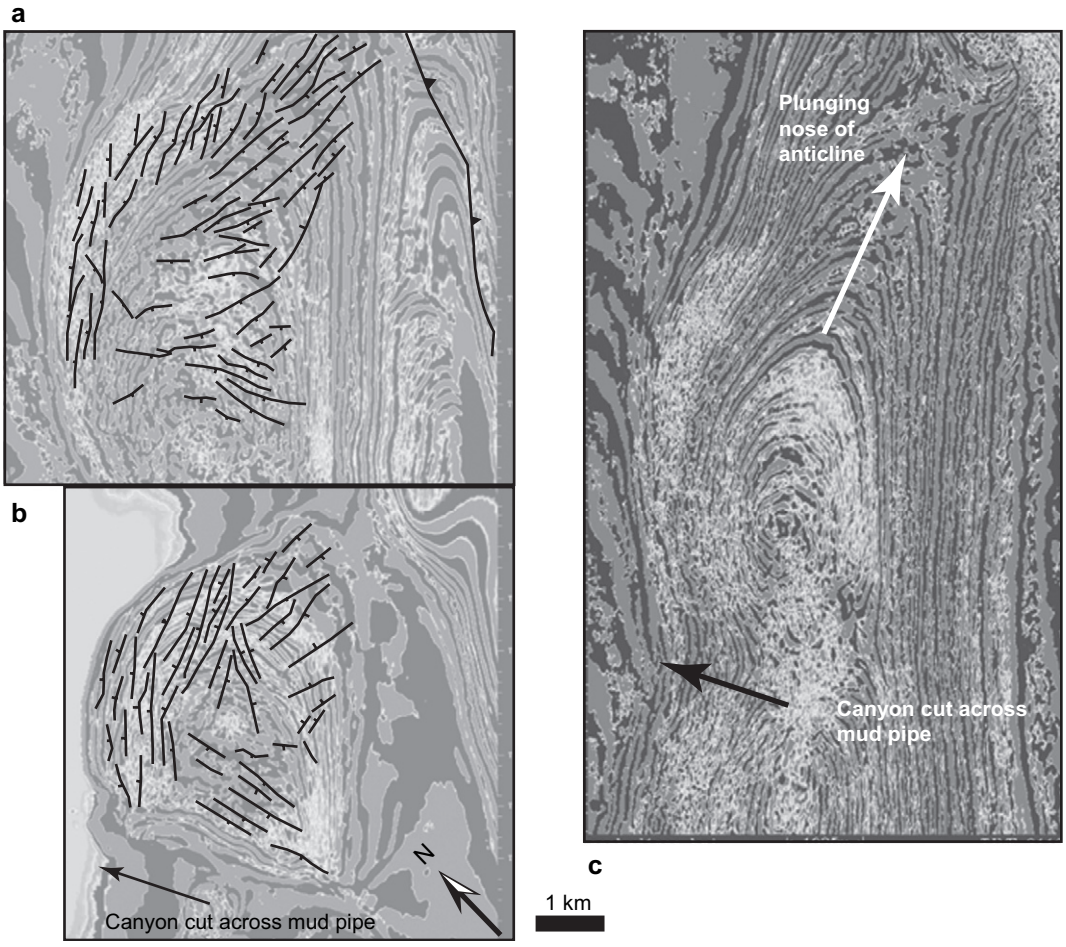

Fig. 16. Time slices across anticline V illustrating the control of surface slope dip direction on fault trends. Surface slope dip can be related to forelimb orientation, canyons and the plunge of anticlines. Time-depths of the time slices are: a, 2820 ms; b, 2544 ms; c, 3116 ms.

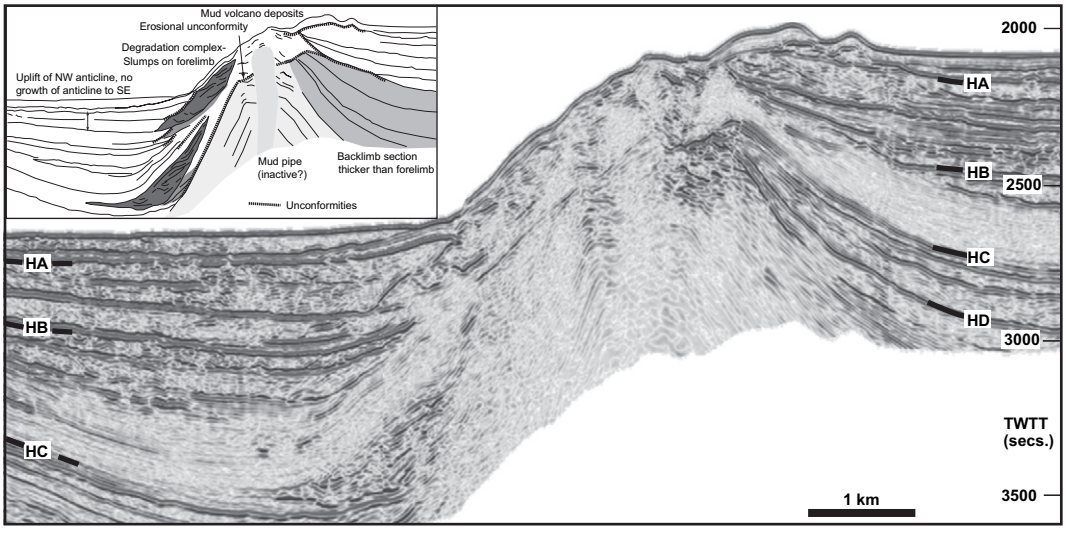

Fig. 17. Seismic line of degradation complex, multiple unconformities and mud pipe, illustrating the very pronounced thinning of section from the back limb to the forelimb. This thinning is in part achieved by wedging and onlap of section onto the back limb, and in part by erosion, mass movement and mass wasting of material from the crest and forelimb of the fold. In part material is re-deposited at the base of the forelimb, giving rise to chaotic deposits, or wedge-shaped units. See Fig. 1 for location. Inset shows the main horizons and other characteristic interpretations.

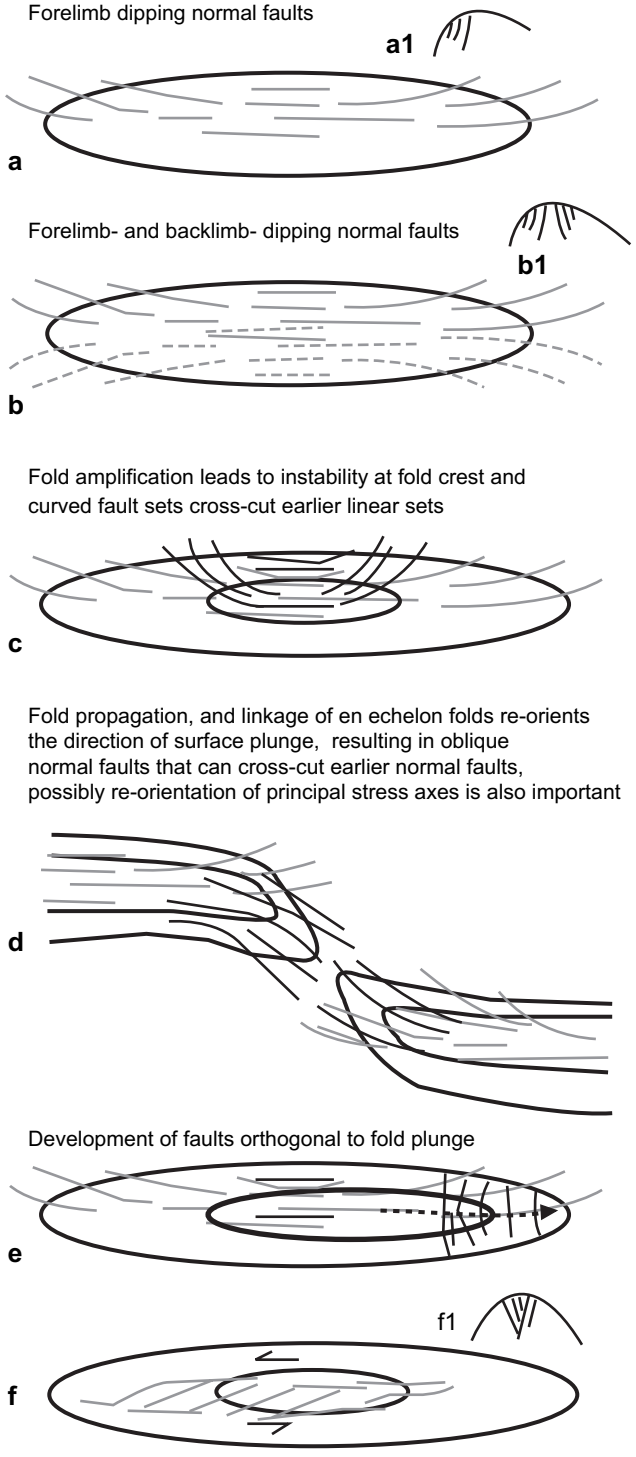

Fig. 18. Schematic illustration of basic map view normal fault geometries with respect to a growing anticline. (a) Foreland dipping normal faults, normal faults tend to curve outwards passing down plunge. (b) Forelimb (solid lines) and back-limb (dashed lines) dipping normal faults. Down plunge the two fault sets tend to diverge. (c) As folds grow instability at the fold crest can promote development of a more arcuate later normal fault set that in places cross-cuts the earlier, more fold axis parallel normal fault set. (d) As two en-echelon folds propagate laterally and start to link, the normal fault sets tend to swing around sub-parallel to the oblique fold trend. These may cross-cut earlier fault sets of pattern (a) above. (e) Normal faults sub-perpendicular to the fold axis cross-cut earlier axis sub-parallel faults where fold amplification produces a fold plunge that has greater dip than the forelimb dip. (f) Normal faults produced by a component of strike-slip motion across the anticline. a1, b1 and f1 illustrate the basic cross-sectional fault geometries associated with each setting. With low back-limb surface dips faults may only develop on the forelimb (a1), gravity (slope) influenced faults will form divergent conjugate fault sets (b1), whilst most commonly normal faults caused by a component of strike-slip along the fault will have a conjugate convergent geometry (f1).

wasting geometry is illustrated in Fig. 21 (inset), which shows two stages of fold development interpreted as fault propagation folds, based on 2D seismic across slope folds (Ping and Liu, 2004). The backlimbs of the more external anticlines (e.g. anticlines VIII and IX Fig. 1) dip at a lower angle (20°) than the more internal anticlines (35°). This difference in dip may in part reflect some folding and back-rotation of older, yet still active thrusts as the fold belt propagated oceanwards. The steeper internal dips may also reflect steepening of the thrust fault as it propagates higher in the section. The simple fold geometry with normal faults developed whilst the thrust fault was blind, the fault tip lying about 0.4 km or deeper in the subsurface.

Fig. 21 shows a graph of fold interlimb angle plotted against average surface slope dip above the anticline, with points coded to represent the different fold styles described above. The graph shows that in general the transition to more intense faulting, and mass movement processes is accompanied by an increase in interlimb angle and in surface slope dip. For the category of simple folds the interlimb angle values are quite widely scattered between 180° and 150°. This is because included in the category are the small (low wavelength) folds high up the continental slope that have relatively low interlimb angles (165–150°), but appear to have been almost continuously buried by sediment during fold growth. Also in the category are the youngest folds in the province, with high interlimb angles (180–170°). Hence crest uplift rate relative to sedimentation rate is an important (but difficult to quantify) factor; the interlimb angle is much easier to quantify. The deep normal faults tend to develop in folds with interlimb angles between 170° and 140°, and where surface slopes are 4–12°. Large rotational slump scars plus normal faulting tend to occur where interlimb angles are smaller than 165° and slope angles are greater than 6°. For degradation complex development surface slope dip does not increase beyond about 12–13°. Instead it is the interlimb angle that increases, indicating that once a critical slope angle is reached mass movement processes remove the crest of the anticline as it continues to tighten.

Withjack and Scheiner (1982) have shown how fault patterns associated with domal uplift are sensitive to domal uplift shape and stress. Despite being composed of planar not listric faults, the curved map-view fault pattern on several anticlines (Figs. 12 and 13) is very reminiscent of rotational slips. In the Withjack and Scheiner (1982) experiments variations in stress state (extensional, strike-slip, thrust) were shown to explain variations in the fault patterns. For the deepwater anticlines local variations in stress orientation are possible (for example near lateral and oblique ramps, at regions of mud pipe intrusion) and could influence fault orientation. This may well be the

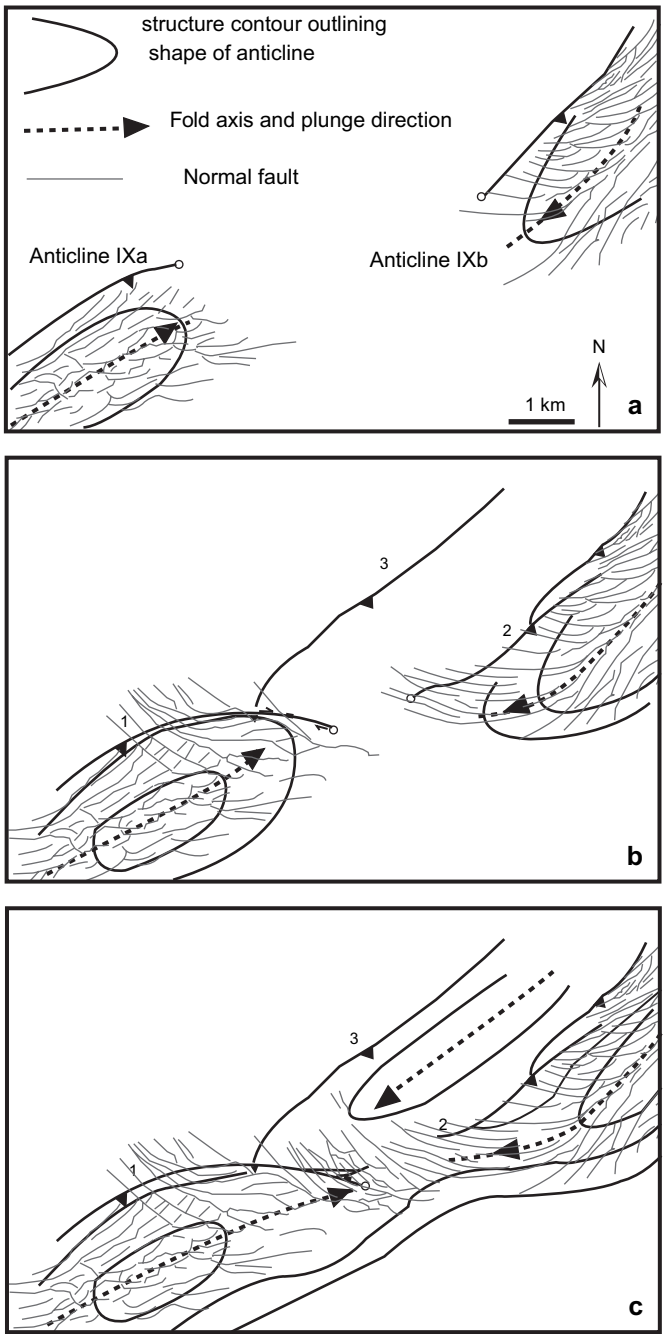

Fig. 19. Evolution of the oblique thrust fault system affecting anticline IX, and associated development of crestal normal fault systems. (a) Early stage where the thrusts 1 and 2 are separated and have begun to propagate towards each other. (b) Intermediate stage where the anticlines associated with thrusts 1 and 2 propagated closer, the NE plunging nose of anticline IXa, generates NW-SE striking normal faults that cross-cut earlier fold axis sub-parallel faults. (c) Anticlines IXa and 1Xb have propagated closer, but link in a broad ~3 km wide saddle (Fig. 12). Whilst the influence of slope dip (i.e. gravity) appears to be an important influence of the fault pattern, local deflection of regional stresses around the oblique fault and fold tips (e.g. Wilkerson et al., 1992; Apotria, 1995) may also be important for controlling the fault orientations in saddle area.

case for some of the geometries discussed in Section 2.4, it is likely that gravitational stress, and local deflection of regional stress (e.g. at propagating fold tips, oblique thrusts; Wilkerson et al., 1992; Apotria, 1995) are interacting at linkage areas of en-echelon folds (Figs. 12, 18d,e and 19). However, most of the range in fault patterns appear to be related to changing slope geometries around folds, both as a consequence of structural geometries (fold plunge Figs. 13b, 16 and 17; en-echelon fold linkage, Fig. 12; oblique ramps in faults, Fig. 13b) and sedimentary processes (canyon development, Fig. 16; slump scar geometry, Fig. 7).

In some ways the development of the anticlines with their faulting and mass wasting effects resembles development of tilted fault blocks in an extensional setting (Fig. 2 anticline VI for example). The syn-kinematic strata evolve from progressively thinning onto the crest to not being deposited at all on the forelimb. Consequently during the later stages of fold growth the distribution of the late syn-kinematic section starts to resemble a large extensional tilted fault block, where the rotated fold backlimb is equivalent to the footwall block, and the crest and forelimb resembles the degraded normal fault scarps that have been described from the North Sea (e.g., Stewart and Reeds, 2003; Figs. 9d and 17).

3. Discussion and conclusions

The normal faults are significant as one of the main responses to the interaction of gravity and fold growth within the syn-kinematic section. They appear to mark an important stage of syn-kinematic fold development when folding initially impacts sea floor topography. They occur during the time when sediments accumulate on top of growing anticlines, and before the stage when anticline crests become eroded by channels, canyons, and mass wasting processes. Crestal normal faults may occur intermittently during fold growth as folds cycle through different stages of development. The normal faults appear to be part of the mass movement process, however they are a relatively deep seated phenomena (terminating between about 200 and 800 m in the subsurface), and are generally not associated with a discrete low-angle basal detachment or slide. Fault geometries in map view range from straight, to anastamosing to highly curved, with complex cross-cutting relationships. These curved geometries are very reminiscent of fault patterns associated with landslips.

Although it is argued here that the normal faults arise primarily due to gravity, other sources of stress probably played a contributing role, either as a widespread feature of the anticlines (outer arc bending stress), or as more local features (e.g. crestal collapse due to mud pipe activity, local development of strike-slip or oblique slip motion across a fold; at oblique fault and fold tips).

Crestal normal faults may be present as single faults or arrays of faults. Generally the number of faults increases as fold interlimb angle increases. Hence along an individual fold, faults are more numerous at the crest and die out down plunge. Across the anticlines with the highest density of normal faults the total summed vertical displacement on all visible fault sets is unlikely to exceed 1 km, or assuming a 60° average fault dip a total of about 610 m heave (13% extension). Faults display a range of geometries in map view that appear to reflect changes in slope dip direction and steepness. Dip-section

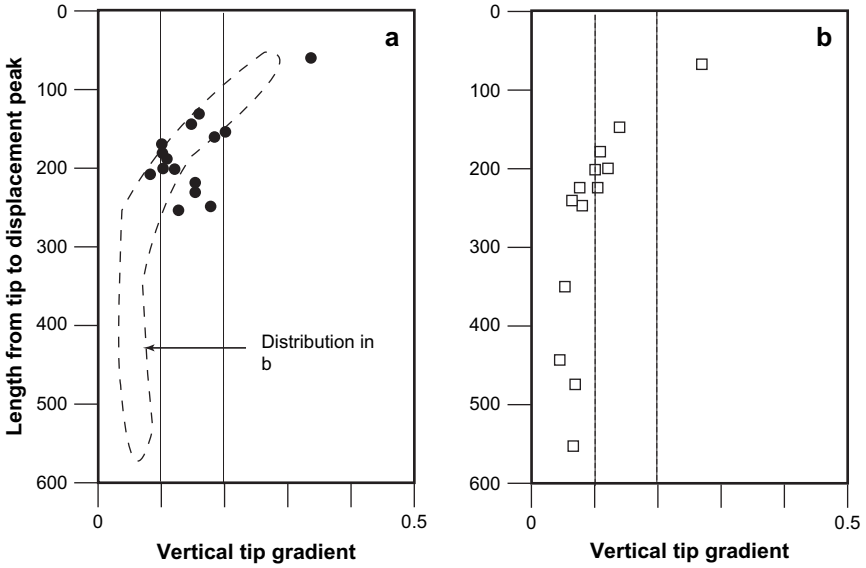

Fig. 20. Difference between tip gradients in dip view for the upper parts of normal faults (a) and the lower parts of normal faults (b) in Fig. 8.

displacement profiles most commonly display asymmetric profiles with the faults losing displacement over shorter distances towards the surface compared to the deep fault tips. This asymmetry may partially reflect easier loss of displacement by transfer of strain to the surrounding rock volume where initial porosities are highest in the rock volume (i.e. the upper 200 m of section).

Normal fault complexes appear to play a significant role in trapping shallow gas, and contribute to the complex shallow geometry of anticline crests. They only appear to affect the upper one second of data, and hence are unlikely to affect hydrocarbon reservoirs, which tend to lie deeper than 1 km. However, perhaps further up the slope, where inactive anticlines are more deeply buried, crestal normal faults are present at depths appropriate for hydrocarbon-bearing reservoirs. They may also be significant in acting as shallow conduits for gas, and providing lateral seals for shallow overpressured sands. The faults are crossed in places by bottom simulating multiples indicative of gas hydrates.

Although the influence of gravity on anticline development has been emphasised here, the normal faults have another potentially important aspect. The faults are transient phenomena, recording the direction of shallow local stress during folding. This local stress tensor is likely to be the sum of stresses of

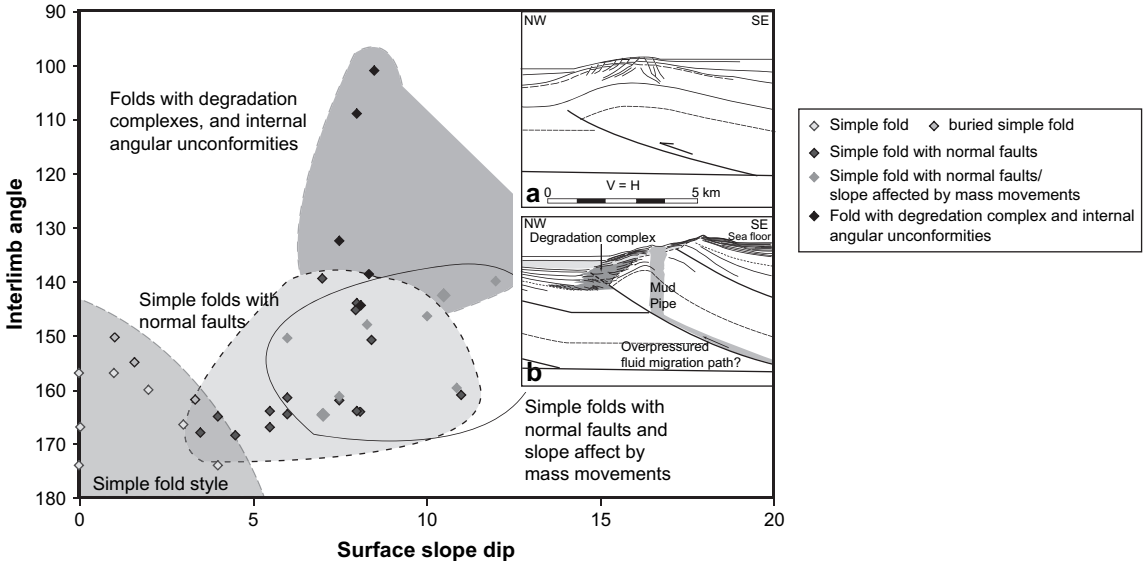

Fig. 21. Fold interlimb angle vs slope dip of seafloor above anticlines, shading indicates the type of associated fold geometry. Note: variation within the simple fold group is affected by fold amplitude and wavelength, not just interlimb angle, because where sedimentation has kept pace with the growth of relatively short-wavelength, low-amplitude folds, the fold crests of relatively tight folds can be buried and consequently are not exposed to mass movement and mass wasting processes. Inset sketches illustrating the differences in maturity between lower slope (a) and middle-upper slope (b) folds. (a) External fold with normal faults, (b) internal fold with degradation complex and mud pipe.

different origins, not just gravity and evolves with fold growth. As the fold develops the normal fault patterns change orientation and cross-cut earlier faults, and thus record such effects as fold amplitude increase, oblique thrust fault development, creation of deep erosional channels, and lateral propagation and linkage of en-echelon folds. In this regard the evolving normal fault pattern may be an important tool for discerning the details of fold evolution, particularly relationships between fold amplitude increase and lateral fold propagation.

Acknowledgements

Ken McCaffrey and Simon Stewart are thanked for constructive reviews that helped improve the manuscript. Thanks to Landmark for providing the software for seismic interpretation software. Arnold Bouma is gratefully acknowledged for comments made to an earlier version of the manuscript.

References

Apotria, T.G., 1995. Thrust sheet rotation and out-of-plane strains associated with oblique ramps: an example from the Wyoming salient, USA. Journal of Structural Geology 17, 647–662.

Bally, A.W., 1989. Atlas of Seismic Stratigraphy. AAPG Studies in Geology 27 (Vol. 3), 243 pp.

Brown, A.R., 1996. Interpretation of Three-Dimensional Seismic Data. AAPG Memoir 42, fourth ed., 423 pp.

Burbank, D.W., McClean, J.K., Bullen, M., Abdrakhmatov, K.Y., Miller, M.G., 1999. Partitioning of intermontaine basins by thrust-related folding, Tien Shan, Kyrgyzstan. Basin Research 11, 75–92, doi:10.1046/j.1365-2117.1999.00086.x.

Burhannudinnur, M., Morley, C.K., 1997. Anatomy of growth faults in poorly lithified sandstones and shales: implications for reservoir studies and seismic interpretation: Part 1 Outcrop study. Petroleum Geoscience 3, 211–224.

Cashman, S., Cashman, K., 2000. Cataclasis and deformation-band formation in unconsolidated marine terrace sand, Humboldt County, California. Geology 28, 111–114.

Castelltort, S., Pochat, S., Van den Driessche, J., 2004. How reliable are growth strata in interpreting short-term (10 s to 100 s ka) growth structure kinematics? Compte Rendus Geoscience 336, 151–158.

Cavin, A., Underwood, M., Fisher, A., Johnston-Karas, A., 2000. Relations between textural characteristics and physical properties of sediments, Northwestern Cascadia basin. In: Fisher, A., Davis, E.E., Escutia, C. (Eds.), Proceedings ODP Scientific Results. 168 (online), available from. http://www-odp.tamu.edu/publications/168_SR/168sr.htm.

Cooper, K.A., Hardy, S., Gawthorpe, R., 2003. Stratigraphic and structural expression of the lateral growth of thrust fault-propagation folds: results and implications from kinematic modelling. Basin Research 15, 165–182, doi:10.1046/j.1365-2117.2003.00203.x.

Colman-Saad, S.P., 1978. Fold development in Zagros simply folded belt, southwest Iran. AAPG Bulletin 62, 984–1003.

Cowie, P.A., Scholz, C.H., 1992. Physical explanation for displacement-length relationship for faults using a post-yield fracture mechanics model. Journal of Structural Geology 14, 1133–1148.

Demyttenacre, R., Tromp, J.P., Ibrahim, A., Allman-Ward, P., Meckel, T., 2000. Brunei deep water exploration from sea floor images and shallow seismic analogues to depositional models in a slope turbidite setting. GCSSEPM Foundation, 20th Bob F. Perkins Annual Research Conference, pp. 304–317.

Ferguson, A., Bouma, A., Santy, L.D., Suliaman, S., 2004. Control of regional and local structural development on the depositional stacking patterns of deepwater sediments in offshore Brunei Darussalam. Indonesian Petroleum Association Conference Abstracts.

Heinio, P., Davies, R.J., 2006. Degradation of compressional fold belts: deepwater Niger Delta. AAPG Bulletin 90, 753–770.

Hinz, K., Schluter, H.U., 1985. Geology of the Dangerous Grounds, South China Sea and the Continental Margin off Southwest Palawan: Results of SONNE Cruises SO-23 and SO-27. Energy 10, 297–315.

Hinz, K., Fritsch, J., Kempter, E.H.K., Mohammad, A.M., Meyer, J., Mohamed, D., Vosberg, H., Weber, J., Benavidez, J., 1989. Thrust tectonics along the north-western continental margin of Sabah/Borneo. Geologisch Rundschau 78, 705–730.

Ingram, G.M., Chisholm, T.J., Grant, C.J., Hedlund, C.A., Stuart-Smith, P., Teasdale, J., 2004. Deepwater North West Borneo: hydrocarbon accumulation in an active fold and thrust belt. Marine and Petroleum Geology 2004, 879–887.

James, D.M.D., 1984. The Geology and Hydrocarbon Resources of Negara Brunei Darussalam. Special Publication, Muzium Brunei and Brunei Shell Petroleum Company Berhad.

McGilvery, T.A., Cook, D.L., 2003. The influence of local gradients on accommodation space and linked depositional elements across a stepped slope profile, offshore Brunei. In: Roberts, H., Rose, N., Fillon, R.H., Anderson, J.B. (Eds.), Shelf Margin Deltas and Linked Down Slope Petroleum Systems: Global Significance and Future Exploration Potential. GCSSEPM Foundation, Bergam et al. Inc., Houston, TX, pp. 387–419.

Nicol, A., Walsh, J.J., Watterson, J., Childs, C., 1996. The shapes, major axis orientations and displacement patterns of fault surfaces. Journal of Structural Geology 18, 235–248.

Nigro, F., Renda, P., 2004. Growth patterns of underlithified strata during thrust-related folding. Journal of Structural Geology 26, 1913–1930.

Ping, Y., Liu, H., 2004. Tectonic-stratigraphic division and blind fold structures in Nansha Waters, South China Sea. Journal of Asian Earth Sciences 24, 337–348.

Ramsay, J.G., 1967. Folding and fracturing of rocks. International Series in the Earth and Planetary Sciences. McGraw-Hill, New York, 568 pp.

Sandal, S.T., 1996. The Geology and Hydrocarbon Resources of Negara Brunei Darussalam: Sybas. Brunei Darussalam, Bandar Seri Begawan, 243 pp.

Stewart, S.A., Davies, R.J., 2006. Structure and emplacement of mud volcano systems in the South Caspian Basin. AAPG Bulletin 90, 771–786.

Stewart, S.A., Reeds, A., 2003. Geomorphology of kilometer-scale extensional fault scarps: factors that impact seismic interpretation. AAPG Bulletin 87, 251–272.

Strayer, L.M., Erickson, S.G., Suppe, J., 2004. Influence of growth strata on the evolution of fault-related folds – distinct element models. In: McClay, K.R. (Ed.), Thrust Tectonics and Hydrocarbon Systems. AAPG Memoir, 82, pp. 413–437.

Walsh, J.J., Watterson, J., 1988. Analysis of the relationship between the displacements and dimensions of faults. Journal of Structural Geology 10, 239–247.

Wilkerson, S.M., Marshak, S., Bosworth, W., 1992. Computerized tomographic analysis of displacement trajectories and three-dimensional fold geometry above oblique thrust ramps. Geology 20, 439–442.

Withjack, M.O., Scheiner, C., 1982. Fault patterns associated with domes- an experimental and analytical study. AAPG Bulletin 66, 302–316.